

Brief Report

Compact and High-Efficiency Liquid-Crystal-on-Silicon for Augmented Reality Displays

Zhenyi Luo ¹, Yuqiang Ding ¹, Fenglin Peng ², Ziqian He ², Yun Wang ² and Shin-Tson Wu ^{1,*} 

¹ College of Optics and Photonics, University of Central Florida, Orlando, FL 32816, USA; zhenyi.luo@ucf.edu (Z.L.); yuqiang.ding@ucf.edu (Y.D.)

² Meta Reality Labs, 9845 Willows Road NE, Redmond, WA 98052, USA; fenglin.peng@meta.com (F.P.); ziqianhe@meta.com (Z.H.); ywang22@meta.com (Y.W.)

* Correspondence: swu@creol.ucf.edu

Abstract: Compact and high efficiency microdisplays are essential for lightweight augmented reality (AR) glasses to ensure longtime wearing comfort. Liquid-crystal-on-silicon (LCoS) is a promising candidate because of its high-resolution density, high brightness, and low cost. However, its bulky illumination system with a polarizing beam splitter (PBS) cube remains an urgent issue to be overcome. To reduce the volume of the LCoS illumination system, here, we propose a compact structure with four thin PBS cuboids. Through simulations, the optical efficiency of 36.7% for an unpolarized input light can be achieved while maintaining reasonably good spatial uniformity. Such a novel design is expected to have a significant impact on future compact and lightweight AR glasses.

Keywords: augmented reality (AR); liquid-crystal-on-silicon; polarizing beam splitter; formfactor; high efficiency

1. Introduction

Augmented reality (AR) and virtual reality (VR) are innovative display technologies with the potential to revolutionize the way we experience the world [1–7]. VR devices immerse users in entirely virtual environments, although video pass-through capabilities can be realized using cameras. AR superimposes digital content onto the real world directly and both virtual and physical objects can be viewed directly, which enables vast applications in education, engineering, training, retail, marketing, navigation, healthcare, etc. [8–12]. AR experiences can be accessed through various devices, including smartphones, tablets, and smart glasses. Among these, the glasses-type ARs are expected to be the optimal choice because of their unparalleled compact form factor, lightweight design, and seamless integration of digital content into the physical world.

AR glasses usually consist of two main components: a light engine for generating digital content and an optical combiner for superimposing the virtual digital content with the real world. Different optical systems have been investigated and employed in prosumer products [13]. Moreover, several promising light engines, such as liquid-crystal-on-silicon (LCoS), LED-on-silicon (different from micro-LED on glass), organic LED, and laser beam scanning, have been developed [14]. Recently, the question of whether LED-on-silicon or LCoS is the superior technology has been the subject of heated debate. Each technology has its own pros and cons. Micro-LED is an emissive display technology that promises to revolutionize visual experiences with high peak brightness, fast response time, true dark state, and long lifetime, but its manufacturability remains to be overcome [15–17]. On the other hand, LCoS is a non-emissive reflective projection display that requires illumination optics [18]. The conventional LCoS system is facing tremendous challenge due to its bulky illumination optics, which often incorporates a polarizing beam splitter (PBS) cube, as shown in Figure 1a. Several approaches have been proposed to dramatically reduce the illumination volume of the LCoS pico-projector [19–21]. However, the optical efficiency is



Citation: Luo, Z.; Ding, Y.; Peng, F.; He, Z.; Wang, Y.; Wu, S.-T. Compact and High-Efficiency Liquid-Crystal-on-Silicon for Augmented Reality Displays. *Photonics* **2024**, *11*, 669.

<https://doi.org/10.3390/photonics11070669>

Received: 8 June 2024

Revised: 30 June 2024

Accepted: 15 July 2024

Published: 17 July 2024



Copyright: © 2024 by the authors. Licensee MDPI, Basel, Switzerland. This article is an open access article distributed under the terms and conditions of the Creative Commons Attribution (CC BY) license (<https://creativecommons.org/licenses/by/4.0/>).

often compromised, and the fabrication process is relatively sophisticated. LCoS design with two PBS films as the illumination optics has been proposed earlier [22]. However, it only reduces the system volume by half, and the illumination uniformity still requires further improvement.

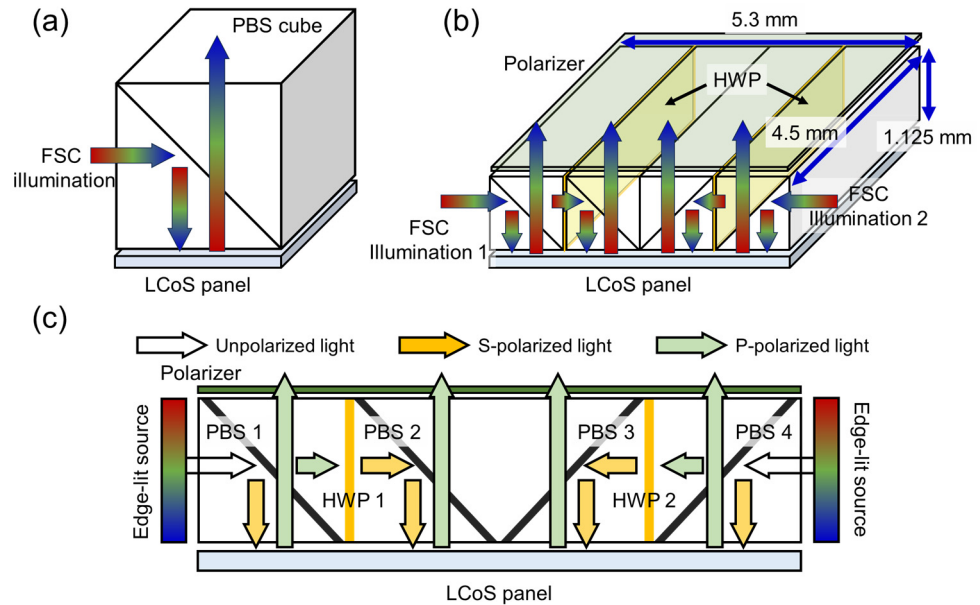


Figure 1. (a) Conventional LCoS illumination optics with a PBS cube. (b) Our proposed compact LCoS projection system with 4 PBS cuboids and 2 HWP films. (c) Polarization control inside the system.

In this paper, we propose a new design for the LCoS illumination system with four thin PBS cuboids to reduce the formfactor. The volume of the proposed illumination system is only 25% of the conventional PBS-based system. The system effectiveness is demonstrated by our simulation results. A reasonably high optical efficiency of 36.7% for an unpolarized light source and good illumination uniformity are achieved.

2. Methods

The proposed compact LCoS system is depicted in Figure 1b,c (side view). Two synchronized edge-lit LED sources provide field sequential color (FSC) illumination to the system. As Figure 1c depicts, the incident unpolarized lights from both left and right edges come from the same mini-LED array, and they are synchronized for FSC operation. For the convenience of discussion, let us assume the PBS 1 and PBS 4 cuboids reflect s-wave (yellow arrows) and transmit p-wave (green arrows). The reflected downward s-wave is modulated by the LCoS panel and converted to p-wave, which in turn transmits through PBS 1 and PBS 4, respectively. The p-wave passing through PBS 1 (and PBS 4) is converted to s-wave by the following half-wave plate HWP 1 (and HWP 2). Subsequently, these s-waves are reflected toward the bottom LCoS panel by the PBS 2 and PBS 3 cuboids, respectively. The reflected beams from the LCoS panel are converted to p-wave and then pass through the PBS 2 and PBS 3 cuboids, respectively. As a result, all the four outgoing beams are p-polarized, as Figure 1c depicts. A sheet polarizer placed on top of the PBS array helps to clean up the polarization state. The output light can be collimated by specifically designed projection optics for AR display applications.

3. Simulations

Ray-tracing simulations were conducted using LightTools software (version 9.1.1) The edge-lit sources provided a uniform angular intensity within ± 20 degrees for the simulations. The LCoS panel size in our simulation was 4 mm by 4 mm, ensuring over 1000 by 1000 pixels since a small LCoS pixel of 4 μm can be achieved nowadays. The total

LCoS reflectance is assumed to be 70% for simulating the bright-state performance [23]. The 90° MTN cell provides a high reflectance of 80% after considering the fringe field effect. Additionally, the reflectance of the bottom pixelated aluminum mirror is about 90%; thus, the total LCoS reflectance is about 70% in our simulations. The four PBS films and two HWPs are immersed in an NBK7 cuboid (length: 5.3 mm, width: 4.5 mm, height: 1.125 mm) through our simulations. The size of the cuboid is slightly larger than the LCoS panel to avoid total internal reflection on the cuboid side surface, as the radiation cone of the reflected light from LCoS panel can be as large as 20 degrees. As Figure 1a depicts, the height needs to be at least 4.5 mm to achieve illumination on the same LCoS panel size with a conventional PBS cube. However, in our four-PBS design, the height is reduced to ¼, i.e., the effective volume is reduced by fourfold.

The optical performance of the compact LCoS system is closely related to the employed polarizing components. PBS films with a multilayer structure as shown in Figure 2a are essential to achieve high-performance near-eye displays. The transmittance and reflectance of the employed PBS films are presented in Figure 2b, which show a high contrast ratio of over 900:1 for the reflection mode and 11,400:1 for the transmission mode. Such high-performance PBS films are commercially available from 3M. The PBS cube includes a PBS film coating sandwiched between two glass prisms. Additionally, the HWPs exhibit excellent achromatic behavior when the incident angle is within ±20°, as illustrated in Figure 2c. The phase retardance gradually decreases as the incident angle increases, which is also beneficial for our system as the reflected light from the LCoS panel may pass through the HWP with a large incident angle. Most of the light after the HWP will keep the original polarization state and will not affect the illumination uniformity seriously. The thickness of the PBS films and HWPs is 0.1 mm in our simulations for more reliable investigation of the illumination uniformity and stray light.

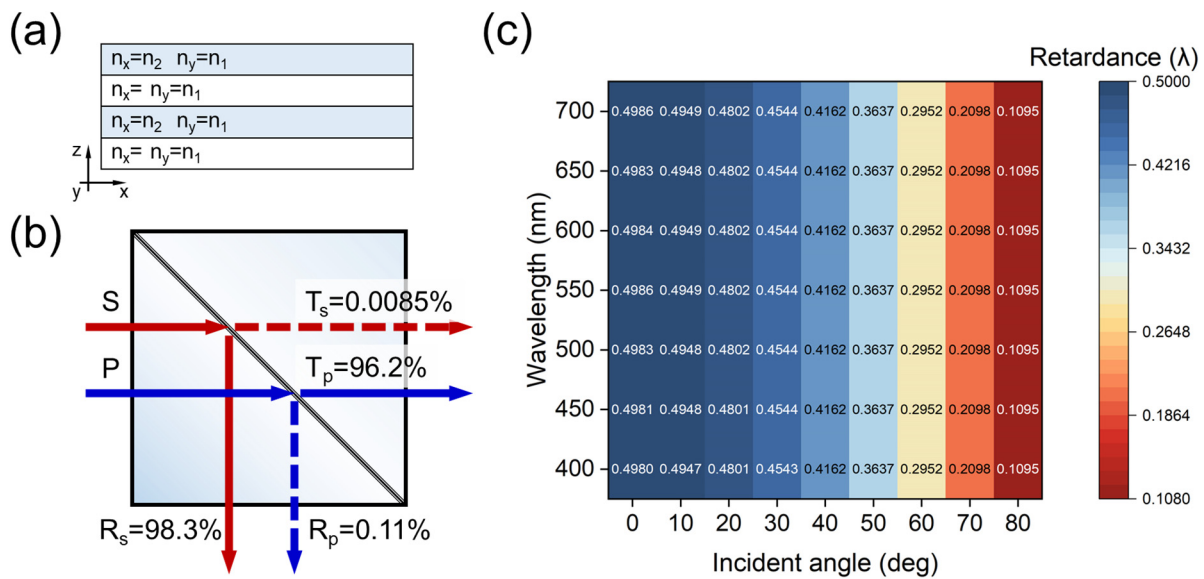


Figure 2. (a) PBS films with multilayer structure. (b) Transmittance and reflectance of the employed PBS films. (c) Phase retardance of the HWPs.

Figure 3a,b show the simulated results for illumination on the LCoS panel. The cross-section diagrams indicate excellent uniformity when $Z = 0$. However, two deep valleys appear in the diagram when $X = 0$. The thickness of the PBS films and HWPs is one reason for the nonuniformity, where the practical optimization is limited. Additionally, the illumination on the LCoS surface originates from the reflection of the PBS films. As Figure 3c shows, there is illumination loss in some incident angles in the vicinities of the HWP. In the current design (Figure 1c), no light appears in the dark red line region.

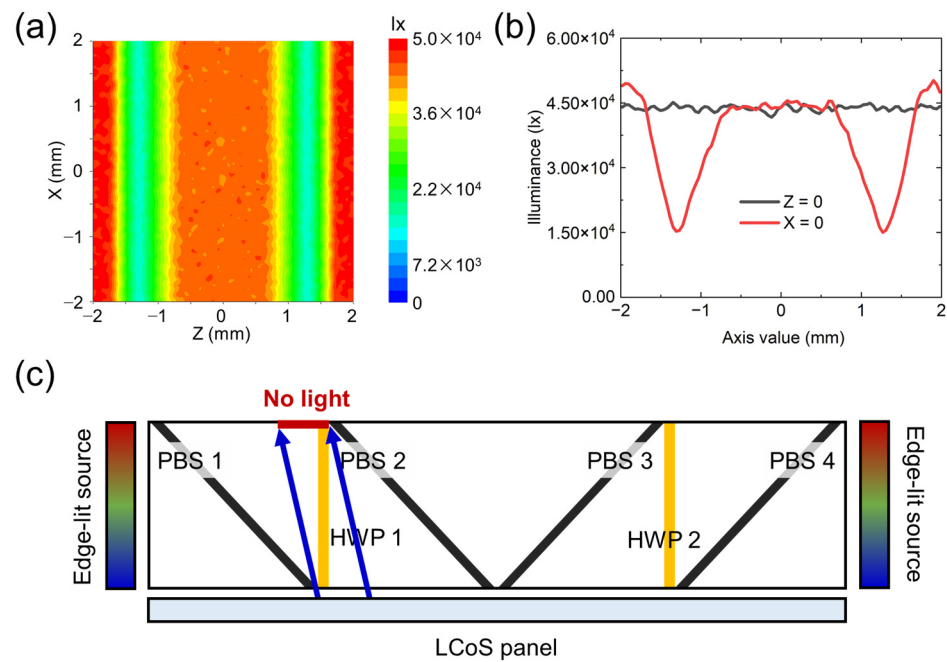


Figure 3. (a) Illumination uniformity at the LCoS surface. (b) Cross-section diagrams of the illumination. (c) Origins of the nonuniformity.

It is worth mentioning that the emission cone of the light source is $\pm 20^\circ$. Blue arrows represent the corresponding propagation direction (around 13.2° with respect to the vertical direction) in the glass for an incident angle of 20° in air. To eliminate the red line region and improve the illumination uniformity on the LCoS surface, we intentionally tilt the orientation of the two HWPs, as shown in Figure 4a. The tilt angle is 15° , which is designed to be larger than the refractive angle (20° in air) of the glass material. The thickness of the PBS films (without the prisms) and HWPs remains 0.1 mm, as mentioned above. The length of the illumination system decreases from 5.3 mm to 4.7 mm due to the shift in the PBS films and HWPs. The width and height of the PBS cuboids remain the same as before (4.5 mm and 1.125 mm, respectively). Figure 4b illustrates the optimized illumination on LCoS surface. According to the cross-sectional diagrams shown in Figure 4c, the illumination uniformity has been significantly improved by tilting the HWP orientation. The ratio of minimum illuminance over maximum illuminance increases from 30% to over 60%. The width of the valleys has also been reduced. Digital modulation can be employed to further improve the uniformity by controlling the polarization states of the reflected light from each pixel on the LCoS panel, which helps to improve the overall uniformity after passing through the clean-up polarizer on the top.

In addition to illumination uniformity, we also studied the full on/off contrast ratio and optical efficiency (represented by the full-on flux because the total luminous flux from the two edge-lit sources is 1 lm). Results are summarized in Table 1. The optical efficiency is increased from 33.9% to 36.7% after tilting the HWPs, while the contrast ratio remains almost the same. For a hybrid AR/VR convertible display, a high contrast ratio is important when the VR mode is used. However, most AR glasses are used under ambient lighting conditions, such as inside a room or outdoors. Even if the employed microdisplay has an infinity contrast ratio, its ambient contrast ratio could be significantly reduced by the stray light inside the housing and the ambient light. Specifically, the ambient luminance is 300 nits on an overcast day while the luminance of the AR glasses is usually around 1000 nits nowadays. Although a good dark state of the LCoS panel is favorable, the ambient contrast ratio of the AR glasses is mainly limited by the ambient lighting conditions; the dark-state performance of the LCoS panel does not make a significant difference.

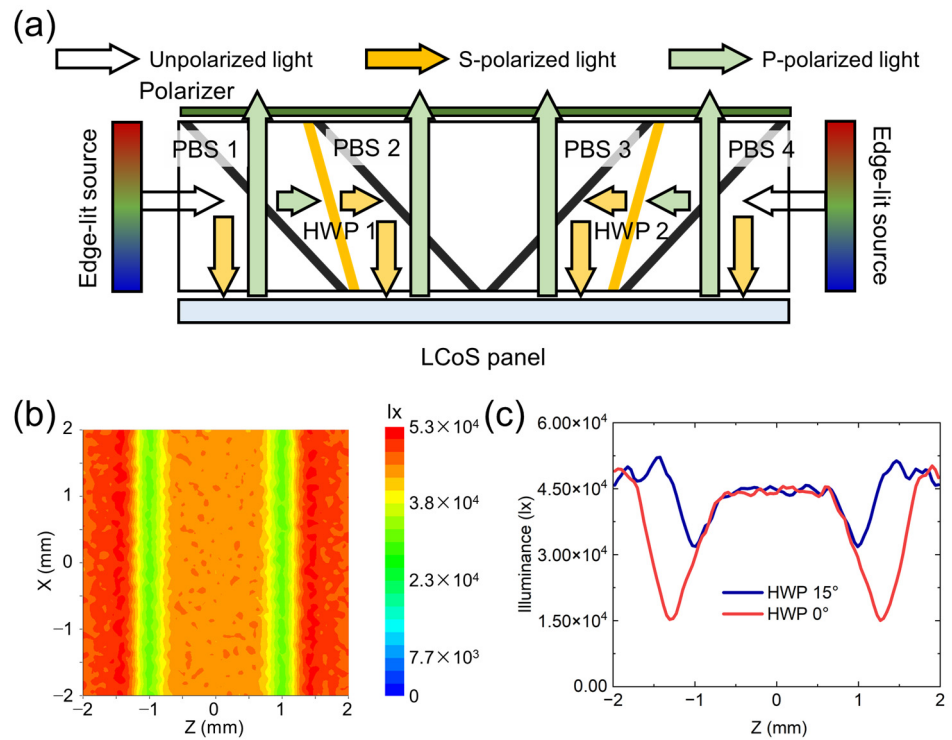


Figure 4. (a) Intentionally tilting the HWPs to optimize the illumination on LCoS surface. (b) Optimized illumination. (c) Cross-section diagrams of HWPs with different tilt angles.

Table 1. Full on/off contrast of different system configurations.

	HWP 0°	HWP 15°
Full on * (lm)	0.33876	0.36715
Full off * (lm)	0.00223	0.00248
Contrast	151.6	148.0

* Luminous flux of full-on state and full-off state is measured after the top polarizer within a maximum incident angle of 20°. The total luminous flux from the two edge-lit sources is 1 lm.

4. Conclusions

A compact and high-efficiency LCoS system has been proposed and demonstrated by our simulations. The novel illumination optics consist of four PBS films with high contrast ratio and two HWPs. These optical films can be coated on the surfaces of the glass components, which will be cemented together to form the illumination system. The incident light from the edge-lit LED array with uniform intensity within ±20° is reflected downwards to the LCoS panel by the PBS films while the HWPs control the polarization states. The HWPs are intentionally tilted to address the nonuniformity issue in the proposed system. The system enables a high optical efficiency of 36.7% after optimizing for uniformity. Additionally, the simple fabrication procedure of our design, which is based on mature optical components, is also favorable for mass production. Offering a slim formfactor, high optical efficiency, and favorable manufacturability, such a novel LCoS system is expected to open a new door for next-generation AR glasses.

Author Contributions: Conceptualization, Z.L. and S.-T.W.; methodology, Z.L., F.P. and Z.H.; simulation, Z.L. and Y.D.; writing—original draft preparation, Z.L.; writing—review and editing, S.-T.W.; supervision, Y.W. and S.-T.W. All authors have read and agreed to the published version of the manuscript.

Funding: The UCF group is indebted to Meta Platforms for the financial support.

Institutional Review Board Statement: Not applicable.

Informed Consent Statement: Not applicable.

Data Availability Statement: The data presented in this study are available from the authors upon reasonable request.

Conflicts of Interest: The authors declare no conflicts of interest.

References

1. Azuma, R.T. A survey of augmented reality. *Presence Teleoperators Virtual Environ.* **1997**, *6*, 355–385. [[CrossRef](#)]
2. Burdea, G.C.; Coiffet, P. *Virtual Reality Technology*; John Wiley & Sons: New York, NY, USA, 2003.
3. Carmigniani, J.; Furht, B.; Anisetti, M.; Ceravolo, P.; Damiani, E.; Ivkovic, M. Augmented reality technologies, systems and applications. *Multimed. Tools Appl.* **2011**, *51*, 341–377. [[CrossRef](#)]
4. Kress, B.C.; Cummings, W.J. Optical architecture of HoloLens mixed reality headset. In Proceedings of the Digital Optical Technologies 2017, Munich, Germany, 25–29 June 2017; Volume 10335, pp. 124–133.
5. Chang, C.; Bang, K.; Wetzstein, G.; Lee, B.; Gao, L. Toward the next-generation VR/AR optics: A review of holographic near-eye displays from a human-centric perspective. *Optica* **2020**, *7*, 1563–1578. [[CrossRef](#)] [[PubMed](#)]
6. Xiong, J.; Hsiang, E.L.; He, Z.; Zhan, T.; Wu, S.-T. Augmented reality and virtual reality displays: Emerging technologies and future perspectives. *Light Sci. Appl.* **2021**, *10*, 216. [[CrossRef](#)] [[PubMed](#)]
7. Yin, K.; Hsiang, E.L.; Zou, J.; Li, Y.; Yang, Z.; Yang, Q.; Lai, P.-C.; Lin, C.-L.; Wu, S.-T. Advanced liquid crystal devices for augmented reality and virtual reality displays: Principles and applications. *Light Sci. Appl.* **2022**, *11*, 161. [[CrossRef](#)] [[PubMed](#)]
8. Wu, H.-K.; Lee, S.W.-Y.; Chang, H.-Y.; Liang, J.-C. Current status, opportunities and challenges of augmented reality in education. *Comput. Educ.* **2013**, *62*, 41–49. [[CrossRef](#)]
9. Webel, S.; Bockholt, U.; Engelke, T.; Gavish, N.; Olbrich, M.; Preusche, C. An augmented reality training platform for assembly and maintenance skills. *Robot. Auton. Syst.* **2013**, *61*, 398–403. [[CrossRef](#)]
10. Poushneh, A.; Vasquez-Parraga, A.Z. Discernible impact of augmented reality on retail customer’s experience, satisfaction and willingness to buy. *J. Retail. Consum. Serv.* **2017**, *34*, 229–234. [[CrossRef](#)]
11. Rauschnabel, P.A.; Felix, R.; Hinsch, C. Augmented reality marketing: How mobile AR-apps can improve brands through inspiration. *J. Retail. Consum. Serv.* **2019**, *49*, 43–53. [[CrossRef](#)]
12. Narzt, W.; Pomberger, G.; Ferscha, A.; Kolb, D.; Müller, R.; Wieghardt, J.; Hörtner, H.; Lindinger, C. Augmented reality navigation systems. *Univers. Access Inf. Soc.* **2005**, *4*, 177–187. [[CrossRef](#)]
13. Ding, Y.; Yang, Q.; Li, Y.; Yang, Z.; Wang, Z.; Liang, H.; Wu, S.-T. Waveguide-based augmented reality displays: Perspectives and challenges. *eLight* **2023**, *3*, 24. [[CrossRef](#)]
14. Hsiang, E.L.; Yang, Z.; Yang, Q.; Lai, P.C.; Lin, C.L.; Wu, S.T. AR/VR light engines: Perspectives and challenges. *Adv. Opt. Photonics* **2022**, *14*, 783–861. [[CrossRef](#)]
15. Lee, V.W.; Twu, N.; Kymissis, I. Micro-LED technologies and applications. *Inf. Disp.* **2016**, *32*, 16–23. [[CrossRef](#)]
16. Huang, Y.; Hsiang, E.-L.; Deng, M.-Y.; Wu, S.-T. Mini-LED, micro-LED and OLED displays: Present status and future perspectives. *Light Sci. Appl.* **2020**, *9*, 105. [[CrossRef](#)] [[PubMed](#)]
17. Chen, P.; Li, Q. 55-4: Invited Paper: Monolithic MicroLED Display for AR Applications. *SID Symp. Dig. Tech. Pap.* **2023**, *54*, 1874–1877. [[CrossRef](#)]
18. Huang, Y.; Liao, E.; Chen, R.; Wu, S.-T. Liquid-Crystal-on-Silicon for Augmented Reality Displays. *Appl. Sci.* **2018**, *8*, 2366. [[CrossRef](#)]
19. Li, Y.-W.; Chen, K.-Y.; Chen, W.-H.; Lin, C.-W.; Wang, C.-T.; Fan-Chiang, K.-H.; Kuo, H.-C.; Tsai, H.-C. 13-1: Invited Paper: Front-lit LCOS for AR Displays. *SID Symp. Dig. Tech. Pap.* **2023**, *54*, 154–517. [[CrossRef](#)]
20. Tang, E. The smallest LCoS engine: Introducing the AG-30L2. In Proceedings of the SPIE AR, VR, MR Industry Talks 2023, San Francisco, CA, USA, 30 January–2 February 2023; Volume 12450, p. 124500O.
21. Luo, Z.; Ding, Y.; Peng, F.; Wei, G.; Wang, Y.; Wu, S.-T. Ultracompact and high-efficiency liquid-crystal-on-silicon light engines for augmented reality glasses. *Opto-Electron. Adv.* **2024**, *7*, 240039. [[CrossRef](#)]
22. Sieler, M.; Schreiber, P.; Foerster, E. Projection Display and Method of Displaying an Overall Picture. U.S. Patent 8,794,770, 5 August 2014.
23. Fan-Chiang, K.-H.; Chen, S.-H.; Wu, S.-T. Diffraction effect on high-resolution liquid-crystal-on-silicon devices. *Jpn. J. Appl. Phys.* **2005**, *44*, 3068. [[CrossRef](#)]

Disclaimer/Publisher’s Note: The statements, opinions and data contained in all publications are solely those of the individual author(s) and contributor(s) and not of MDPI and/or the editor(s). MDPI and/or the editor(s) disclaim responsibility for any injury to people or property resulting from any ideas, methods, instructions or products referred to in the content.